

A NEW CONSTRAINT ON THE ESCAPE FRACTION IN DISTANT GALAXIES USING γ -RAY BURST AFTERGLOW SPECTROSCOPY

HSIAO-WEN CHEN¹, JASON X. PROCHASKA^{2,3}, AND NICKOLAY Y. GNEDIN^{4,1,5}

Submitted to the Astrophysical Journal Letters

ABSTRACT

We describe a new method to measure the escape fraction f_{esc} of ionizing radiation from distant star-forming galaxies using the afterglow spectra of long-duration γ -ray bursts (GRBs). Optical spectra of GRB afterglows allow us to evaluate the optical depth of the host ISM, according to the neutral hydrogen column density $N(\text{HI})$ observed along the sightlines toward the star-forming regions where the GRBs are found. Different from previous effort in searching for faint, transmitted Lyman continuum photons, our method is not subject to background subtraction uncertainties and does not require prior knowledge of either the spectral shape of the host galaxy population or the IGM Ly α forest absorption along these GRB sightlines. Because most GRBs occur in sub- L_* galaxies, our study also offers the first constraint on f_{esc} for distant low-mass galaxies that dominate the cosmic luminosity density. We have compiled a sample of 28 GRBs at redshift $z \gtrsim 2$ for which the underlying $N(\text{HI})$ in the host ISM are known. These GRBs together offer a statistical sampling of the integrated optical depth to ionizing photons along random sightlines from star-forming regions in the host galaxies, and allow us to estimate the mean escape fraction $\langle f_{\text{esc}} \rangle$ averaged over different viewing angles. We find $\langle f_{\text{esc}} \rangle = 0.02 \pm 0.02$ and place a 95% c.l. upper limit $\langle f_{\text{esc}} \rangle \leq 0.075$ for these hosts. We discuss possible biases of our approach and implications of the result. Finally, we propose to extend this technique for measuring $\langle f_{\text{esc}} \rangle$ at $z \sim 0.2$ using spectra of core-collapse supernovae.

Subject headings: cosmology:observations—gamma-rays:bursts—galaxies:high-redshift—galaxies:ISM

1. INTRODUCTION

Observations of distant QSOs indicate that the intergalactic medium (IGM) became fully ionized by redshift $z \sim 6$ (e.g. Fan, Carilli, & Keating 2006). While at $z < 3$ QSOs are the dominant sources of the ultraviolet background radiation (e.g. Haardt & Madau 1996), at higher redshifts where the number density of QSOs declines steeply toward earlier epochs (e.g. Willott et al. 2005; 2005; Richards et al. 2006) additional ionizing sources are necessary. The spectral shape of the ultraviolet background radiation inferred from intervening metal absorption line studies (e.g. Haehnelt et al. 2001) and intergalactic He II absorption spectra (e.g. Shull et al. 2004; Reimers et al. 2005) suggest that young stars may provide the dominant ionizing sources during early epochs.

The escape fraction of ionizing radiation, f_{esc} , specifies the fraction of stellar-origin ionizing photons ($h\nu > 1$ Ryd) that escape the interstellar medium (ISM) of star-forming galaxies. Accurate measurements of f_{esc} are important for quantifying the relative contribution of ionizing photons to the ultraviolet background radiation between galaxies and AGN. For the Milky Way, estimates based on diffuse H α emission of High Velocity Clouds (HVC) yield an upper limit of $f_{\text{esc}} \lesssim 6\%$ (e.g. Bland-Hawthorn & Maloney 1999 and see Weiner et al. 2001

for a review). In the nearby universe, early observations of starburst galaxies place constraints at $f_{\text{esc}} \lesssim 6\%$ (e.g. Heckman et al. 2001). Bergvall et al. (2006) have reported the first positive detection of Lyman continuum photons in the spectra of the starburst galaxy Haro 11 using the *Far-UV Space Explorer*. Their analysis suggests an escape fraction in this galaxy of $f_{\text{esc}} = 1 - 10\%$. This finding has, however, been challenged by Grimes et al. (2007), who cannot confirm the detection of Lyman continuum in the same data set.

At higher redshift, a range of values are reported from $f_{\text{esc}} < 6\%$ at $z = 1.1 - 1.4$ (Malkan et al. 2003; Siana et al. 2007), to between mean values of no more than 8% (Giallongo et al. 2002; Fernández-Soto et al. 2003; Shapley et al. 2006) and $f_{\text{esc}} \approx 13 - 38\%$ (Inoue et al. 2005) at $z \sim 3$, to $f_{\text{esc}} \approx 22\%$ at $\langle z \rangle = 3.4$ (Steidel et al. 2001)⁶. In addition, direct detections of Lyman continuum photons are reported for two $z \sim 3$ galaxies by Shapley et al. (2006), implying $f_{\text{esc}} \approx 13 - 20\%$ for these two sources. The large scatter in the reported f_{esc} may imply a large variation in the optical depth across different lines of sight toward the inner regions of the galaxies (e.g. Gnedin, Kravtsov, & Chen 2007), but it also underscores the challenges in detecting low-luminosity features in a background noise limited regime.

In this *Letter*, we describe a novel approach for constraining f_{esc} from high-redshift star-forming galaxies. We estimate f_{esc} based on the distribution of neutral hydrogen column density $N(\text{HI})$ observed in the afterglow spectra of long-duration γ -ray bursts (GRBs). Long-

⁶ Note that many of the previous publications reported measurements for $f_{\text{esc,rel}}$, which is defined as the ratio of escaped ionizing photons at 912 Å to the observed flux density at 1500 Å. Here we have converted these relative measurements to f_{esc} at 1 Ryd based on their respective $\langle E(B - V) \rangle$ reported by the authors.

¹ Department of Astronomy & Astrophysics, University of Chicago, Chicago, IL 60637, USA, hchen@oddjob.uchicago.edu

² University of California Observatories - Lick Observatory, University of California, Santa Cruz, CA 95064, USA; xavier@ucolick.edu

³ Department of Astronomy and Astrophysics, University of California, Santa Cruz, CA 95064, USA

⁴ Particle Astrophysics Center, Fermi National Accelerator Laboratory, Batavia, IL 60510, USA; gnedin@fnal.gov

⁵ Kavli Institute for Cosmological Physics, University of Chicago, Chicago, IL 60637, USA

duration GRBs are believed to originate in the death of massive stars with $M > 20 M_{\odot}$ (see Woosley & Bloom 2006 for a recent review), and are signposts of active star-forming regions in the ISM of their host galaxies (e.g. Bloom et al. 2002; Fruchter et al. 2006). Spectroscopic observations of the bright optical afterglows following the initial bursts have allowed us to measure the gas and dust content along the sightlines toward the GRBs, based on absorption features imprinted in the afterglow spectra (e.g. Vreeswijk et al. 2004; Chen et al. 2005; Prochaska et al. 2007a). These GRB sightlines together offer a statistical sampling of the integrated optical depth to ionizing photons along random directions in the host galaxies.

The escape fraction f_{esc} determined from the $N(\text{HI})$ distribution along random sightlines in the ISM of GRB host galaxies does not require direct detection of Lyman continuum photons. It is not subject to systematic uncertainties due to background subtraction. The f_{esc} value is derived based on the total gas column observed in front of the star-forming region that hosts the GRB. It does not depend on the spectral shape of the ultraviolet radiation from the host galaxy or the stochastic uncertainties in the IGM Ly α forest absorption along the lines of sight. Finally, while some GRB host galaxies are reported to have high star formation rate, $\text{SFR} \gtrsim 100 M_{\odot}$, (c.f. Berger et al. 2003; Le Flocc'h et al. 2006), growing evidence indicates that the majority are sub- L_* galaxies (e.g. Le Flocc'h et al. 2003; Sollerman et al. 2005; Fruchter et al. 2006). Our study therefore offers the first constraint on f_{esc} for low-mass galaxies at $z > 2$.

2. THE SAMPLE OF GRBS AT $Z \gtrsim 2$

To obtain an accurate estimate of the mean escape fraction of ionizing photons along GRB sightlines, we first compile a sample of GRBs that are confirmed at $z \gtrsim 2$. We focus our analysis on bursts at $z_{\text{GRB}} \gtrsim 2$ for two main reasons. First, it minimizes the ambiguity between an optically thin sightline and a low-redshift interloper. The $z > 2$ IGM will imprint its signature on an optical spectrum via the Ly α forest and metal-line absorption features. Therefore, an afterglow that exhibits a featurless spectrum is most likely at $z_{\text{GRB}} < 2$. Second, measurements of $N(\text{HI})$ from the absorption profiles of Ly α and Lyman series allow us to directly evaluate the optical depth at the Lyman limit frequency τ_{LL} .

Table 1 lists 40 spectroscopically confirmed GRBs at $z_{\text{GRB}} \gtrsim 2$. In addition to the redshift of each source, we also list the isotropic equivalent energy release in γ -ray photons (E_{iso}), the observed $N(\text{HI})$ if available, a flag f_{α} to indicate whether the afterglow spectrum covers the redshifted Ly α transition ('0' means no coverage and '1' means Ly α coverage), and a flag f_i to indicate whether metal-line features due to low ions such Si II or C II are present. Four of the GRBs do not have spectral coverage of the Ly α transition from the host, but the presence of low ions (f_i) indicate that the gas is consistent with being optically thick. To exhibit strong low-ion absorption, an optically thin gas would need to have very high density (to maintain a non-negligible neutral fraction) and super-solar metallicity, both of which are very unlikely. Nine sources do not have published $N(\text{HI})$. In the subsequent analysis, we consider only those 28 sightlines with published $N(\text{HI})$ values as our main sample, and assume that the remaining 13 sources with no available

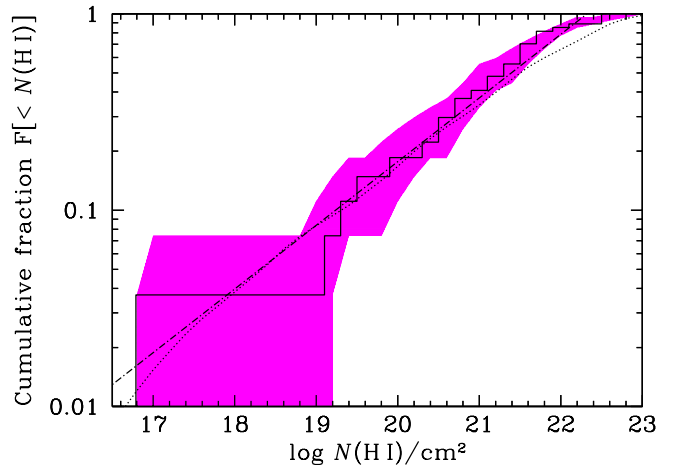


FIG. 1.— Cumulative distribution of neutral hydrogen column density $\mathcal{F}[< N(\text{HI})]$ observed in the host galaxies of long-duration GRBs at $z \geq 2$ (solid histogram). The shaded area shows the $1\text{-}\sigma$ uncertainties evaluated using a bootstrap re-sampling method that accounts for both $N(\text{HI})$ measurement uncertainties and sampling errors. The dash-dotted line represents the best-fit power-law model described in § 3. The dotted curve represents the predicted distribution from Gnedin, Kravtsov, & Chen (2007).

$N(\text{HI})$ measurements share the same distribution as the main sample. This is justified based on the similar z_{GRB} and E_{iso} distributions between GRB sightlines with and without known $N(\text{HI})$ measurements.

Figure 1 presents the cumulative $N(\text{HI})$ distribution, $\mathcal{F}[< N(\text{HI})]$ from the main sample of 28 GRB host galaxies, together with the $1\text{-}\sigma$ uncertainties determined based on a bootstrap re-sampling method. Specifically, we establish a simulated sample of 28 sightlines from random sampling of the main sample, allowing duplications of individual sightlines. Then, we evaluate the cumulative $N(\text{HI})$ distribution of the simulated sample. We repeat the procedure 10,000 times to determine the 68% scatter of \mathcal{F} around the mean value in each $N(\text{HI})$ bin.

3. THE METHOD

The optical depth of Lyman limit photons along individual lines of sight is determined according to $\tau_{\text{LL}} = \sigma_{\text{LL}} \times N(\text{HI})$, where $\sigma_{\text{LL}} = 6.28 \times 10^{-18} \text{ cm}^2$ is the photo-ionization cross section of hydrogen atoms. In principle, *considering a sample of random sightlines from the star-forming regions in a galaxy together yields an estimate of the optical depth averaged over all viewing angles.* In practice, we consider an ensemble of random sightlines toward GRBs in distant star-forming galaxies. The mean escape fraction of Lyman limit photons averaged over all directions is evaluated according to

$$\langle f_{\text{esc}} \rangle = \frac{1}{n} \sum_{i=1}^{i=n} \exp[-\sigma_{\text{LL}} N_i(\text{HI})], \quad (1)$$

where the sum extends over the total number of n GRB sightlines in the sample. For our main sample presented in Figure 1, we find $n = 28$ and Equation (1) yields $\langle f_{\text{esc}} \rangle = 0.02 \pm 0.02$. The error is estimated using the bootstrap re-sampling method described in § 2 and rep-

resents the 68% uncertainty in the mean value. We also determine a 95% c.l. upper limit $\langle f_{\text{esc}} \rangle \leq 0.075$.

Parameterizing the cumulative $N(\text{HI})$ distribution by $\mathcal{F}[< N(\text{HI})] = A [N(\text{HI})/N_0]^\alpha$, we find based on a χ^2 analysis $\log A = -0.58 \pm 0.05$ and $\alpha = 0.32 \pm 0.03$ for $\log N_0 = 20.5$ over $\log N(\text{HI}) = 16.5 - 21.5$ (dash-dotted line in Figure 1). Equation (1) is expressed as

$$\begin{aligned} \langle f_{\text{esc}} \rangle &= \int_0^\infty dN_{\text{HI}} \frac{d\mathcal{F}}{dN_{\text{HI}}} \exp[-\sigma_{\text{LL}} N(\text{HI})] \\ &= \frac{A\alpha}{(\sigma_{\text{LL}} N_0)^\alpha} \Gamma(\alpha). \end{aligned}$$

We determine $\langle f_{\text{esc}} \rangle = 0.020 \pm 0.003$, where the errors represent the 68% uncertainties.

4. DISCUSSION

We have applied the $N(\text{HI})$ measured from the Ly α (and in some cases Lyman series as well) absorption strength in early-time afterglow spectra to constrain the mean escape fraction in distant star-forming galaxies. Different from conventional methods to search for transmitted Lyman continuum photons, our estimated $\langle f_{\text{esc}} \rangle$ is not subject to background subtraction uncertainties and does not depend on the intrinsic ultraviolet spectral shape of the host galaxies or dust distribution in the host ISM. In addition, it does not depend on the stochastic IGM Ly α absorption along the sightlines toward these GRBs. Here we discuss possible biases in our estimated $\langle f_{\text{esc}} \rangle$ due to the selection of GRB sightlines and implications of our result.

4.1. Observational Biases

Our analysis considers only galaxies that host a GRB event. The presence of a GRB indicates that the ISM immediately surrounding the burst is photo-ionized by the bright afterglow. The intensity of the afterglow ionizing radiation is capable of photo-ionizing all H I gas to a distance of $r = 10$ to 30 pc (Drain & Hao 2002; Watson et al. 2007; Prochaska et al. 2007b) that can exceed the typical Stromgren radius of an H II region. It is conceivable that the presence of a GRB may reduce τ_{LL} along the sightline and the constraint on $\langle f_{\text{esc}} \rangle$ can be considered as an upper limit.

In addition, our constraint is derived explicitly at the 912-Å Lyman limit transition. Additional absorption due to dust would further reduce the estimated $\langle f_{\text{esc}} \rangle$, but is almost negligible at frequencies beyond 1 Ryd (see Gnedin et al. 2007). However, some fraction of the GRB afterglows are optically “dark” and missed in our sample because afterglow spectroscopy was impossible. While the majority of these are presumably associated with high- z events (where the IGM absorbs most of the optical photons) or intrinsically faint afterglows, the remainder are associated with highly dust-extinguished sightlines (e.g. Pellizza et al. 2006; Rol et al. 2007). These extremely dusty sightlines are optically thick to ionizing radiation further strengthening the $\langle f_{\text{esc}} \rangle$.

Intrinsically faint UV afterglows could occur in a particularly low-density environment (Kumar & Panaitescu 2000) and, in turn, preferentially probe optically thin sightlines. We note, however, that there is no notable correlation between the observed $N(\text{HI})$ and the afterglow UV luminosity. For example, GRB 021004 and

GRB 050820 have very different $N(\text{HI})$ but comparable afterglow UV luminosity (e.g. Lazzati et al. 2006; Vestrand et al. 2006). Furthermore, the isotropic equivalent energies of the GRB sample (E_{iso} in Table 1) display a wide dispersion at all redshift, supporting that these GRBs do not preferentially originate in low-density environment (e.g. Piran 1999). We argue that the pre-selection of bright UV afterglows has not restricted the analysis to a special sub-sample of GRBs.

4.2. Implications and Future Work

The association between GRBs and massive stars that typically have a short lifetime indicates that the GRB events occur close to the locations where their progenitor stars were formed and directly trace the current star formation rate. Late-time imaging surveys to search for the host galaxies of long-duration GRBs have shown that these GRBs occur in sub- L_* galaxies (Le Flocc’h et al. 2003; Sollerman et al. 2005; Fruchter et al. 2006) that exhibit on average large specific star-formation rates, SFR/L_B , (Christensen et al. 2004). This can be understood as low-mass galaxies undergoing early generations of star formation (Erb et al. 2006). The derivation of f_{esc} from GRB sightlines reveals the escape fraction during the lifetime of the most intense ionizing sources, and applies to ‘normal’, star-forming galaxies that dominates the cosmic UV luminosity density. The low-mass nature also allows a direct comparison with predictions from high-resolution cosmological simulations (the dotted curve in Figure 1; Gnedin et al. 2007).

Our 95% c.l. upper limit of $\langle f_{\text{esc}} \rangle$ is comparable to the low values previously reported based on observations of Lyman continuum photons from more luminous star-forming galaxies at $z \sim 3$ (Giallongo et al. 2002; Fernández-Soto et al. 2003; Shapley et al. 2006). Additional absorption due to dust would further reduce the estimated $\langle f_{\text{esc}} \rangle$, but is almost negligible at frequencies beyond 1 Ryd (see Gnedin et al. 2007). We estimate the total contribution of ionizing photons from sub- L_* galaxies, adopting the UV luminosity function determined for luminous star-forming galaxies at $z \sim 3$ from Adelberger & Steidel (2000). We derive a co-moving luminosity density at 1500 Å of $2.2 \times 10^{26} h \text{ erg s}^{-1} \text{ Hz}^{-1} \text{ Mpc}^{-3}$ for sub- L_* ($0.1 - 1 L_*$) galaxies⁷. Applying an extinction correction to the observed 1500-Å flux (the authors estimated $f_{\text{esc}}(1500\text{Å}) \approx 0.2$) and assuming an intrinsic flux ratio between rest-frame 1500 Å and 900 Å of $f(1500)/f(900) = 3$ adopted by Steidel et al. 2001 (but see Siana et al. 2007), we estimate a co-moving emissivity at 1 Ryd from sub- L_* galaxies of $< 2.8 \times 10^{25} h \text{ erg s}^{-1} \text{ Hz}^{-1} \text{ Mpc}^{-3}$ for the 95% c.l. upper limit $\langle f_{\text{esc}} \rangle \lesssim 0.075$. To estimate the QSO contribution to the ultraviolet background radiation, we adopt the $z = 3$ QSO luminosity function estimated by Hopkins et al. (2007). We find that the contribution to the ionizing background from QSOs of bolometric luminosity $L_{\text{bol}} > 10^8 L_\odot$ is $\approx 5 \times 10^{24} h \text{ erg s}^{-1} \text{ Hz}^{-1} \text{ Mpc}^{-3}$. While the uncertainties in these various numbers are large, this exercise shows that QSOs and sub- L_* galaxies with $\langle f_{\text{esc}} \rangle = 1 - 2\%$ can contribute a comparable amount of ionizing photons to the ultraviolet background radiation at $z \sim 3$.

⁷ We adopt a Λ cosmology, $\Omega_M = 0.3$ and $\Omega_\Lambda = 0.7$, with a dimensionless Hubble constant $h = H_0/(100 \text{ km s}^{-1} \text{ Mpc}^{-1})$.

A larger sample of GRB sightlines with known $N(\text{HI})$ measurements for the host ISM is needed for improving the uncertainties in $\langle f_{\text{esc}} \rangle$. In addition, follow-up imaging surveys for unvailing the emission properties of the GRB host galaxies are valuable for testing model predictions of star formation at high redshift. Specifically, cosmological simulations show that low-mass galaxies are inefficient in emitting ionizing radiation (Gnedin et al. 2007). The luminosity distribution of these GRB hosts offers a direct test of these models.

Finally, it is worth exploring whether a similar analysis could be performed with core-collapse supernovae (SN). These events also trace the death of massive stars over a broader mass range and provide a bright probe of the optical depth through the host galaxy. While the extreme line-blanketing in the far-ultraviolet of SN spectra may preclude the study of Hydrogen absorption, it may be

plausible to pursue an analysis of ISM metal-absorption, e.g. via the Mg II doublet. Indeed, the *HST* spectrum of the Type II SN 1999em shows narrow absorption lines of Fe II, Mg II, and Mg I (Baron et al. 2000). These features imply that NGC 1637 is optically thick to ionizing radiation along this particular sightline. A survey of $z \gtrsim 0.2$ SN could be carried out with a modest resolution, blue-sensitive spectrometer on a 10 m-class telescope.

The authors acknowledge helpful discussion with J. O’Meara, E. Ramirez-Ruiz and M. Dessauges-Zavadsky. We thank A. Kann and J. Bland-Hawthorn for valuable input. H.-W.C. acknowledges support from NASA grant NNG 06GC36G and an NSF grant AST-0607510. J. X. P. acknowledges support from NASA/Swift grant NNG 05GF55G and a CAREER grant (AST-0548180).

REFERENCES

- Adelberger, K. L. & Steidel, C. C. 2000, *ApJ*, 544, 218.
 Baron, E. et al. 2000, *ApJ*, 545, 444.
 Berger, E. et al. 2003, *ApJ*, 588, 99
 Berger, E. 2006, GRB Coordinates Network, 5962, 1.
 Berger, E. & Gladders, M. 2006, GRB Coordinates Network, 5170, 1.
 Berger, E. et al. 2006a, GRB Coordinates Network, 4815, 1.
 Berger, E. et al. 2006b, *ApJ*, 642, 979.
 Berger, E., Fox, D. B., & Cucchiara, A. 2007, GRB Coordinates Network, 6470, 1.
 Bergvall, N. et al. 2006, *A&A*, 448, 513.
 Bland-Hawthorn, J., & Maloney, P. R. 1999, *ApJ*, 510, L33
 Bloom, J. S., Kulkarni, S. R., & Djorgovski, S. G. 2002, *AJ*, 123, 1111.
 Bloom, J. S., Frail, D. A., & Kulkarni, S. R. 2003, *ApJ*, 594, 674.
 Castro, S. M. et al. 2000, GCN Report 605.
 Castro, S. et al. 2003, *ApJ*, 586, 128.
 Cenko, S. B. et al. 2006, GRB Coordinates Network, 5155, 1.
 Chen, H.-W. et al. 2005, *ApJ*, 634, L25.
 Christensen, L., Hjorth, J., & Gorosabel, J. 2004, *A&A*, 425, 913.
 Cucchiara, A. et al. 2006, High-Resolution Spectroscopy of the Afterglow of GRB 060210, in *Swift and GRBs: Unveiling the Relativistic Universe*, poster
 D’Elia, V. et al. 2006, GRB Coordinates Network, 5637, 1.
 Draine, B. T. & Hao, L. 2002, *ApJ*, 569, 780.
 Erb, D. K. et al. 2006, *ApJ*, 647, 128.
 Fan, X., Carilli, C. L., & Keating, B. 2006, *ARA&A*, 44, 415
 Fernández-Soto, A., Lanzetta, K. M., & Chen, H.-W. 2003, *MNRAS*, 342, 1215.
 Fruchter, A. S. et al. 2006, *Nature*, 441, 463.
 Fynbo, J. P. U. et al. 2006a, GRB Coordinates Network, 5809, 1.
 Fynbo, J. P. U. et al. 2006b, *A&A*, 451, L47.
 Giallongo, E. et al. 2002, *ApJ*, 568, L9
 Gnedin, N. Y., Kravtsov, A. V., & Chen, H.-W. 2007, *ApJ* submitted (arXiv:0707.0879).
 Grimes, J. P. et al. 2007, *ApJ* in press (arXiv:0707.0693).
 Haardt, F. & Madau, P. 1996, *ApJ*, 461, 20.
 Haehnelt, M. G. et al. 2001, *ApJ*, 549, L151.
 Heckman, T. M. et al. 2001, *ApJ*, 558, 56.
 Hjorth, J. et al. 2003, *ApJ*, 597, 699.
 Hopkins, P. F., Richards, G. T., & Hernquist, L. 2007, *ApJ*, 654, 731
 Inoue, A. K. et al. 2005, *A&A*, 435, 471.
 Jakobsson, P. et al. 2004, *A&A*, 427, 785.
 Jakobsson, P. et al. 2006, *A&A*, 460, L13.
 Jakobsson, P. et al. 2007, GRB Coordinates Network, 6283, 1.
 Jaunsen, A. O. et al. 2007, GRB Coordinates Network, 6010, 1.
 Kawai, N. et al. 2006, *Nature*, 440, 184.
 Kumar, P., & Panaitescu, A. 2000, *ApJ*, 541, L51
 Lazzati, D. et al. 2006, *MNRAS*, 372, 1791
 Le Floch, E. et al. 2003, *A&A*, 400, 499.
 Le Floch, E., Charmandaris, V., & Forrest, W. J. 2006, *ApJ*, 642, 636
 Malkan, M., Webb, W., & Konopacky, Q. 2003, *ApJ*, 598, 878.
 Pellizza, L. J. et al. 2006, *A&A*, 459, L5.
 Piran, T. 1999, *Phys. Rep.*, 314, 575
 Piranomonte, S. et al. 2006, GRB Coordinates Network, 4520, 1.
 Piranomonte, S. et al. 2007, *A&A* in press (arXiv:0704.1729).
 Price, P. A. et al. 2007, *ApJ*, 663, L57
 Prochaska, J. X. et al. 2007a, *ApJS*, 168, 231.
 Prochaska, J. X. et al. 2007b, *ArXiv Astrophysics e-prints*.
 Quimby, R. et al. 2005, GRB Coordinates Network, 4221, 1.
 Reimers, D., Fechner, C., Hagen, H.-J., et al. 2005, *A&A*, 442, 63
 Richards, G. T. et al. 2006, *AJ*, 131, 49.
 Rol, E. et al. 2006, GRB Coordinates Network, 5555, 1.
 Rol, E. et al. 2007, *ApJ* submitted (arXiv:0706.1518)
 Ruiz-Velasco, A. E. et al. 2007, *ApJ* in press (arXiv:0706.1257)
 Sakamoto, T. et al. 2005, *ApJ*, 629, 311.
 Savaglio, S. et al. 2007, GRB Coordinates Network, 6166, 1.
 Shapley, A. E. et al. 2006, *ApJ*, 651, 688.
 Shin, M.-S. et al. 2007, *ApJ* submitted (astro-ph/0608327).
 Shull, J. M. et al. 2004, *ApJ*, 600, 570.
 Siana, B. et al. 2007, arXiv:0706.4093.
 Sollerman, J. et al. 2005, *New Astronomy*, 11, 103.
 Steidel, C. C., Pettini, M., & Adelberger, K. L. 2001, *ApJ*, 546, 665.
 Thoene, C. C. et al. 2007a, GRB Coordinates Network, 6379, 1.
 Thoene, C. C. et al. 2007b, GRB Coordinates Network, 6499, 1.
 Vestrand, W. T. et al. 2006, *Nature*, 442, 172
 Vreeswijk, P. M. et al. 2004, *A&A*, 419, 927.
 Vreeswijk, P. M. et al. 2006, *A&A*, 447, 145.
 Watson, D. et al. 2006, *ApJ*, 652, 1011.
 Watson, D. et al. 2007, *ApJ*, 660, L101.
 Weiner, B. J., Vogel, S. N., & Williams, T. B. 2002, in *ASP Conf. Ser. 254, Extragalactic Gas at Low Redshift*, ed. J. S. Mulchaey & J. Stocke (San Francisco: ASP), 256
 Willott, C. J. et al. 2005, *ApJ*, 626, 657.
 Woosley, S. E. & Bloom, J. S. 2006, *ARA&A*, 44, 507.

TABLE 1
THE SAMPLE OF GRBS AT $z \geq 2$

GRB	z_{GRB}	$\log E_{\text{iso}}^{\text{a}}$	$\log N(\text{HI})$	f_{α}^{b}	f_{i}^{c}	Ref.
000301c	2.03	52.64	21.2 ± 0.5	1	7	1
000926	2.04	53.76	21.30 ± 0.25	1	7	2
011211	2.14	53.17	20.4 ± 0.2	1	7	3
020124	3.20	52.81	21.7 ± 0.4	1	7	33
021004	2.33	52.82	19.5 ± 0.5	1	3	4
030226	1.99	53.20	20.5 ± 0.3	1	7	34
030323	3.37	52.99	21.90 ± 0.07	1	7	5
030429	2.65	52.87	21.6 ± 0.2	1	7	6
050319	3.24	52.81	20.9 ± 0.2	1	7	22
050401	2.90	53.94	22.6 ± 0.3	1	7	7
050505	4.27	53.81	22.05 ± 0.10	1	7	8
050730	3.97	53.76	22.15 ± 0.10	1	7	9
050820	2.61	53.61	21.1 ± 0.1	1	7	10
050904	6.29	54.32	21.3 ± 0.2	1	7	11
050908	3.34	52.65	19.1 ± 0.1	1	3	4
050922c	2.19	52.73	21.55 ± 0.10	1	7	12
051109	2.34	52.89	...	0	1	13
060115	3.53	53.28	...	1	7	14
060124	2.30	53.39	19.3 ± 0.2	1	3	4
060206	2.26	52.45	20.85 ± 0.1	1	7	15
060210	3.91	53.99	21.7 ± 0.2	1	7	16
060223	4.41	53.06	...	1	7	17
060510b	4.94	53.96	21.1 ± 0.1	1	7	18
060522	5.11	53.42	20.5 ± 0.5	1	7	19
060526	3.21	52.67	20.0 ± 0.2	1	3	20
060605	3.78	52.73	...	1	3	21
060607	3.08	53.27	16.85 ± 0.10	1	3	4
060707	3.42	53.20	21.0 ± 0.2	1	7	22
060714	2.71	53.20	21.8 ± 0.1	1	7	22
060906	3.68	53.38	21.85 ± 0.1	1	7	22
060908	2.43	53.07	...	0	1	23
060926	3.20	52.24	22.7 ± 0.1	1	7	24
060927	5.47	53.49	22.5 ± 0.4	1	7	25
061110b	3.44	53.08	...	1	7	26
061222b	3.35	53.29	...	0	1	27
070110	2.35	52.78	...	1	7	28
070411	2.59	53.07	...	1	1	29
070506	2.31	51.88	...	1	7	30
070529	2.50	53.05	...	0	1	31
070611	2.04	52.01	...	1	1	32

NOTE. — References: 1. Castro et al. (2000); 2. Castro et al. (2003); 3. Vreeswijk et al. (2006); 4. Prochaska et al. in preparation; 5. Vreeswijk et al. (2004); 6. Jakobsson et al. (2004); 7. Watson et al. (2006); 8. Berger et al. (2006b); 9. Chen et al. (2005); 10. Prochaska et al. (2007a); 11. Kawai et al. (2006); 12. Piranomonte et al. (2007); 13. Quimby et al. (2005); 14. Piranomonte et al. (2006); 15. Fynbo et al. (2006b); 16. Cucchiara, Fox & Berger (2006); 17. Berger et al. (2006a); 18. Price et al. (2007); 19. Cenko et al. (2006); 20. Berger & Gladders (2006); 21. Savaglio et al. (2007); 22. Jakobsson et al. (2006); 23. Rol et al. (2006); 24. D’Elia et al. (2006); 25. Ruiz-Velasco et al. (2007); 26. Fynbo et al. (2006a); 27. Berger (2006); 28. Jaunsen et al. (2007); 29. Jakobsson et al. (2007); 30. Thoene et al. (2007a); 31. Berger et al. (2007); 32. Thoene et al. (2007b); 33. Hjorth et al. (2003); 34. Shin et al. (2007).

^aIsotropic equivalent energy release of γ -ray photons (erg s^{-1}). For pre-*Swift* bursts, the energy interval corresponds to 200 – 2000 keV (Bloom et al. 2003; Sakamoto et al. 2005). For *Swift* bursts (2005 and on), the energy interval corresponds to 10 – 150 keV, and no k-corrections have been applied.

^b f_{α} : flag for available Ly α coverage in the afterglow spectra: 0 = No coverage; 1 = Ly α coverage.

^c f_{i} : cumulative flag describing the properties of the ISM surrounding the GRB: 1 = presence of low ions (e.g. Si II, C II); 2 = the gas is optically thick at the Lyman limit; 4 = The Ly α absorption strength indicates $N(\text{HI}) > 2 \times 10^{20} \text{ cm}^{-2}$. For example, a $\text{flag}_{\text{ISM}} = 7$ indicates the system is a DLA with associated low ions.